AGU PUBLICATIONS

Geophysical Research Letters

Supporting Information

for

"*Spatiotemporal Variations in Surface Heat Loss Imply a Heterogeneous Cooling History for the Mantle*"

by

Krister S. Karlsen[1*], Clinton P. Conrad[1], Mathew Domeier[1] and Reidar G. Trønnes[1,2]

[1] Centre for Earth Evolution and Dynamics, University of Oslo, Norway
[2] Natural History Museum, University of Oslo, Norway
* k.s.karlsen@geo.uio.no

Contents of This File

- Text S1, S2
- Figures S1, S2, S3, S4, S5, S6

Introduction

The supporting information in this document contains an extended methodology section (Text S1), a summary of relevant observations and data associated with the assembly and breakup of Pangea (Text S2), and six figures (Figs. S1-S6) that support claims made in the main text.

Text S1: Methods

Generating Seafloor Age Grids

Karlsen et al. (2020) developed a code (http://doi.org/10.5281/zenodo.3687548) that generates seafloor age grids from plate tectonic reconstructions. We used this software to produce age grids from the present-day back to 400 Ma using the updated plate model of Matthews et al. (2016), which includes corrections for the Pacific after Torsvik et al. (2019).

Calculating Heat Flow

We divide the surface of the Earth into grid cells (0.5 degree resolution). Because Matthews et al. (2016) provides the reconstructed locations of continents, and Karlsen et al. (2020) provides seafloor ages, each cell is at a given point in time (400 Ma to present) defined as either a continent cell or seafloor cell. A seafloor cell has a crustal age τ associated with it, while a continent cell does not. The heat flow from a continent cell is calculated as 6 TW divided by the total continental area at the time. The heat flow $q(\tau)$ from a seafloor cell is calculated after Hasterok (2013) as:

$$q(\tau) = \begin{cases} 506.7\, \tau^{-1/2}, & \tau \le 48.1\, Myr \\ 53 + 106\, e^{-0.034607\, \tau}, & \tau > 48.1\, Myr \end{cases}$$

The result is a global grid, where every cell has a heat flow value assigned to it (Fig. 1a). The total continental heat flow (Q_{cont}) is 6 TW by our definition, but the total oceanic heat flow (Q_{ocean}) is calculated by integrating over the ocean basin area.

Separation into Hemispheres

We approximate the Pacific and African mantle domains as two hemispheres, separated by the 60° W and 120°E meridians (see Fig. 1a and 2). These meridians approximately follow the circumpolar belt of seismically-observed slab material in the mantle, which delineates a curtain of downwelling flow in the mantle that separates the two hemispheres and prevents heat transfer between them (Torsvik et al., 2016). To calculate the mantle heat loss associated with each of these two domains, we integrate the surface heat loss grid (Fig. 1a) over each hemisphere separately. Since we do not know the time-dependent spatial distribution of the surface heat loss associated with plumes (3 TW), we add 1.5 TW to each hemisphere's surface heat loss. We denote the heat loss from each of the mantle domains Q_{Pac} and Q_{Af}. Thus, Q_{Pac} and Q_{Af} each contain contributions from both oceanic and the continental heat loss, as well as half the global plume heat flux. Time-variations in Q_{Pac} and Q_{Af} are plotted in Fig. 3a.

Calculating Mantle Cooling

Based on the mantle heat budget described in Section 3 we can calculate the cooling rates (K/Gyr, defined as positive when the mantle is cooling, Fig. 3b) of the whole mantle following

$$dT/dt = (Q_{ocean} + Q_{cont} + Q_{hotspots} - Q_{radio} - Q_{core})/(m\, c),$$

and for each of the two hemispheres

$$dT/dt = (Q_{Pac} - \tfrac{1}{2} Q_{radio} - \tfrac{1}{2} Q_{core})/(\tfrac{1}{2} m\, c),$$

and

$$dT/dt = (Q_{Af} - \tfrac{1}{2} Q_{radio} - \tfrac{1}{2} Q_{core})/(\tfrac{1}{2} m\, c).$$

Here, c = 1250 J/(K kg) and $m = 4.01 \cdot 10^{24}$ kg. Note that heat contributions related to radiogenic heating and core-mantle heat flow are assumed evenly distributed between the two hemispheres. To obtain mantle cooling curves relative to the present-day (Fig. 3c), the cooling rate curves dT/dt are integrated backwards in time from 0 Ma to 400 Ma.

Text S2: Pangea Assembly and Breakup

While the Pacific domain was almost entirely covered by oceanic lithosphere generated by rapidly spreading mid-ocean ridges for the last 350 Ma (Fig. 1a), the African hemisphere included abundant continental lithosphere and was characterized by the assembly and breakup of Pangea. The assembly of Pangea followed the subduction of large ocean basins and major orogenic events associated with continental collision. This contaminated the asthenosphere of the African mantle domain with metasomatised mantle wedge material and detached continental lithosphere and lower continental crust. The sinking slabs of oceanic lithosphere would have contaminated deeper parts of the sub-Pangean mantle. The chemical imprints of such material are seen in both ocean island basalts (Doucet et al., 2020) and mid-ocean ridge basalts (Meyzen et al., 2007) of the African hemisphere, most notably in the DUPAL region of the south Atlantic and Indian basins (Hart et al., 1984).

The elevated thickness of old oceanic crust close to the passive margins in the African hemisphere may result from a combination of more fertile sources and an elevated mantle potential temperature. Both factors were probably important during continental rifting and early spreading along the Central Atlantic ridge from 195 Ma, along the South Atlantic, Southwest Indian and Central Indian ridges from about 130 Ma, as well as along the Labrador Sea, Baffin Bay and NE Atlantic ridges after 62-54 Ma (Torsvik and Cocks, 2017; Jones et al., 2017). Continental break-up and incipient oceanic spreading caused upwelling and extensive melting of enriched and hot asthenosphere, stemming from the assembly of, and subsequent thermal insulation by, Pangea. The eruption of large igneous provinces (LIPs), which instigated rifting and oceanic spreading, partly preceded and partly accompanied the breakup. In this context, the important LIPs are: the Central Atlantic Magmatic Province (201 Ma), Karoo-Ferrar (183 Ma), Parana-Etendeka (134 Ma), Rajmahal (118 Ma), South (114 Ma) and Central (100 Ma) Kerguelen, the Agulhas Plateau (100 Ma), Marion-Madagascar (87 Ma) and the North Atlantic Igneous Province (62 Ma) (Torsvik et al., 2020). The plume heads associated with these LIP events distributed fertile and hot mantle material laterally over long distances, commonly exceeding 1000 km. Although the main LIP activity mostly preceded the early generation of oceanic crust, some of the fertile and hot plume head material was likely incorporated into the asthenosphere, and may have contributed to the thick oceanic crust.

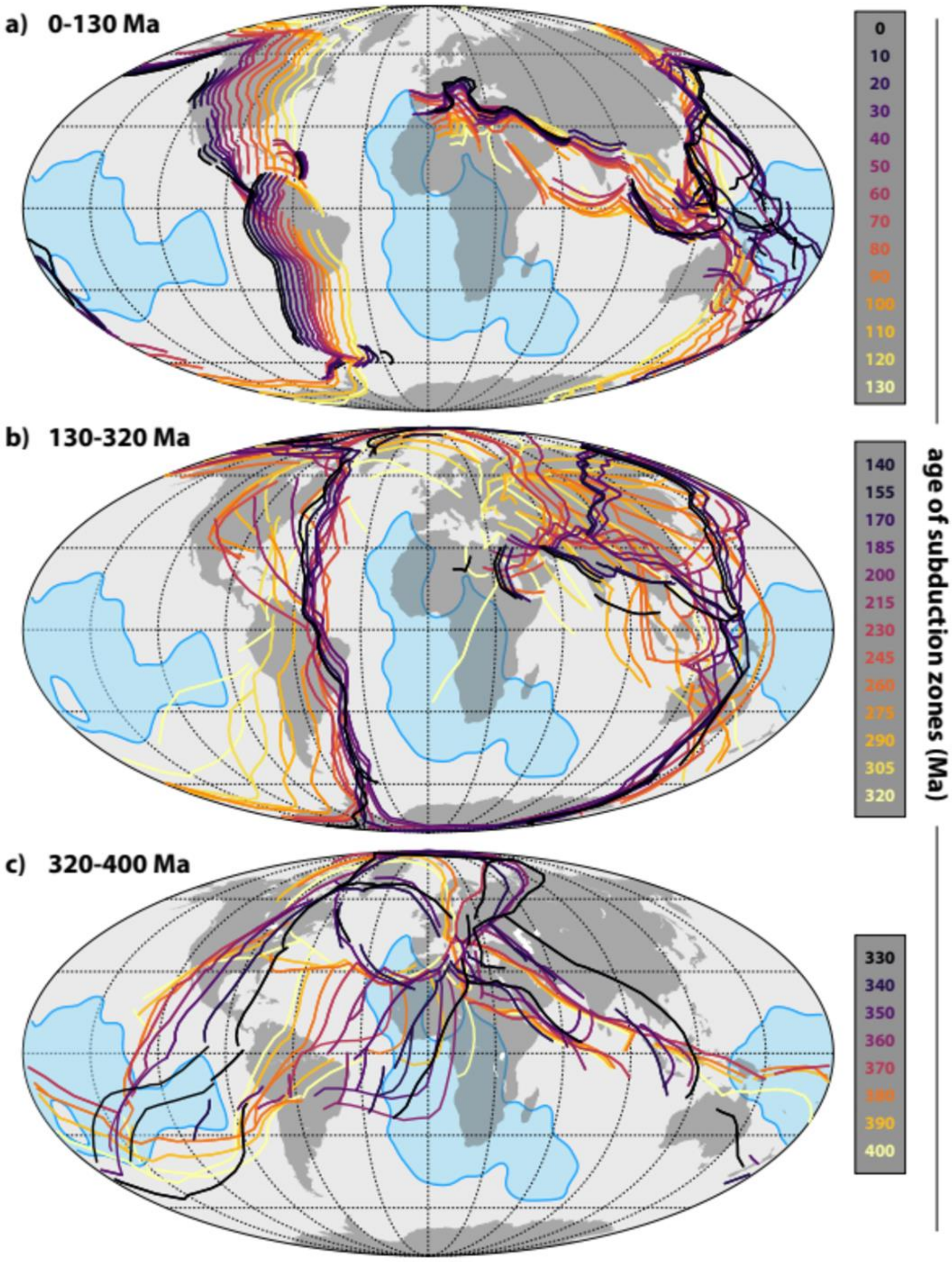

Figure S1: Reconstructed subduction zones through time, draped on the present-day geography and position of the large low shear velocity provinces (LLSVPs) of the lowermost mantle (blue polygons). Reconstructed subduction zones are from the model of Matthews et al. (2016), in the mantle reference frame. *a)* 0-130 Ma: time for which longitude is determinable from hotspot tracks. *b)* 140-320 Ma: less well-constrained paleogeography back to Pangea assembly (~320 Ma); longitude is assumed by holding Africa fixed in longitude. *c)* 320-400 Ma: pre-Pangea assembly, even less well-constrained paleogeography; longitude estimations are based on the plume generation zone method that assumes the LLSVPs to be fixed.

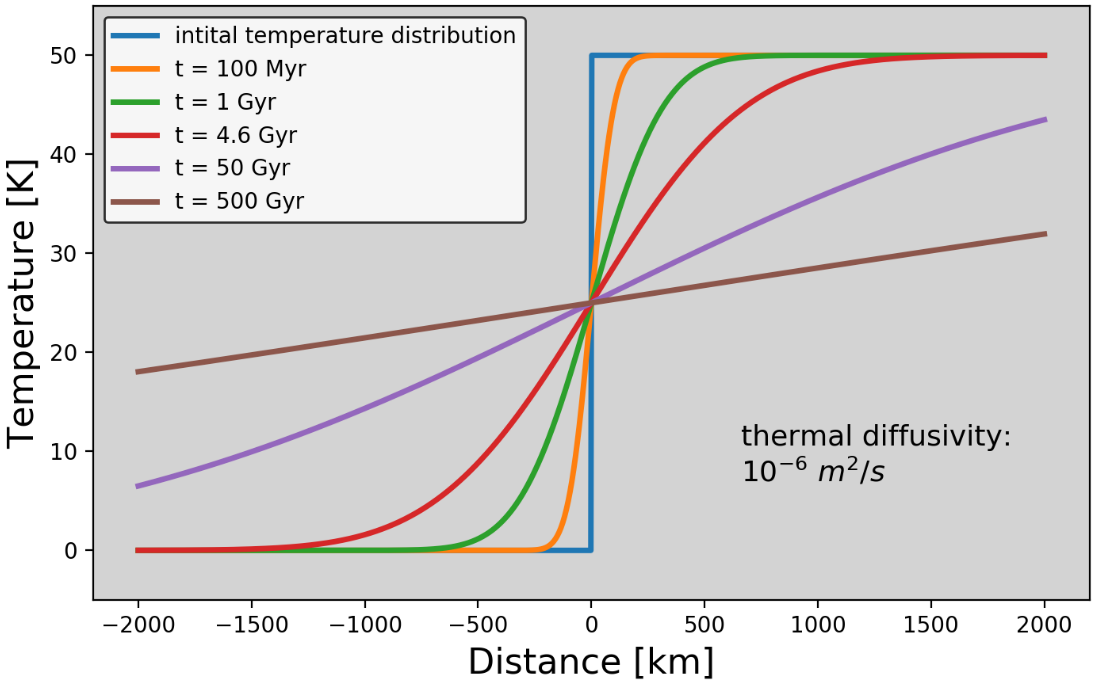

Figure S2: The evolution of a 50 K temperature jump over geologic time based on an analytical solution to the heat equation with a step-function as an initial condition (blue line), see e.g. Stüwe (2002). We note that it takes several times the age of the Earth for a 50 degree temperature jump to smooth by pure conduction across ~10^3 km spatial scales.

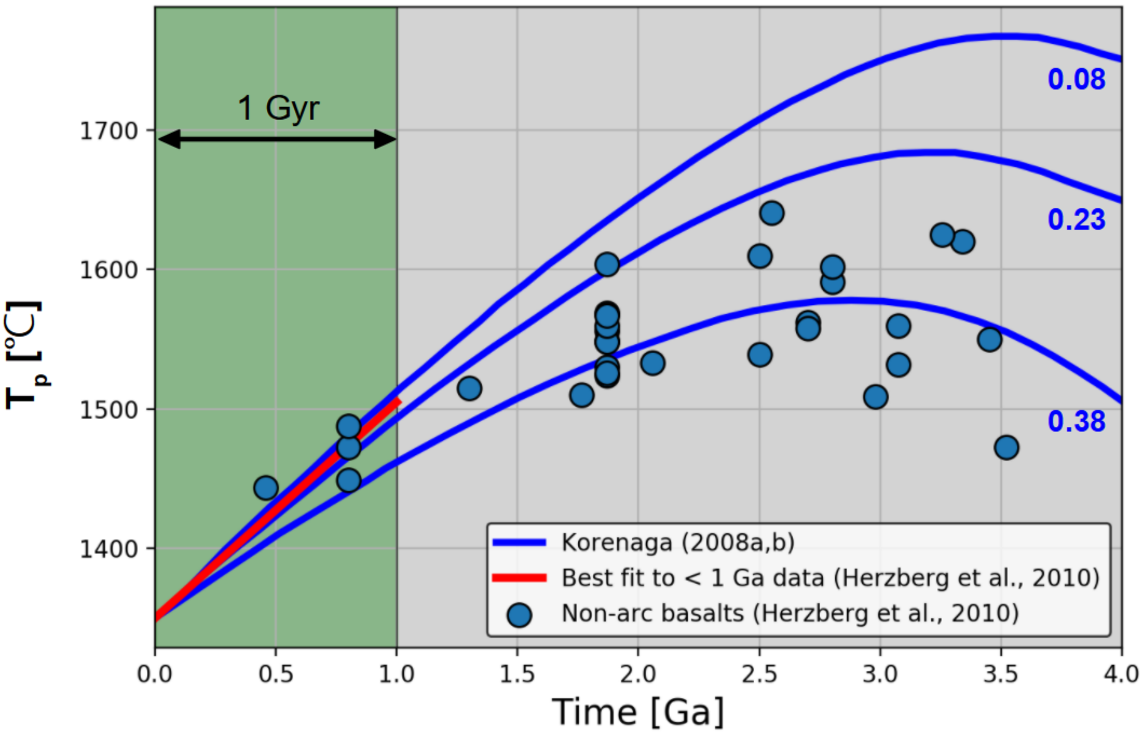

Figure S3: Ambient mantle cooling models and data. Blue curves show mantle cooling models for different present-day Urey ratios, after Korenaga (2008a,b). Dots indicate petrological estimates of mantle potential temperature from non-arc lavas (Herzberg et al., 2010). The red line indicates best the fitting straight line (least squares fit) to the petrological estimates of mantle potential temperature for the past 1 Gyr. The slope of the red line is 155 K/Gyr.

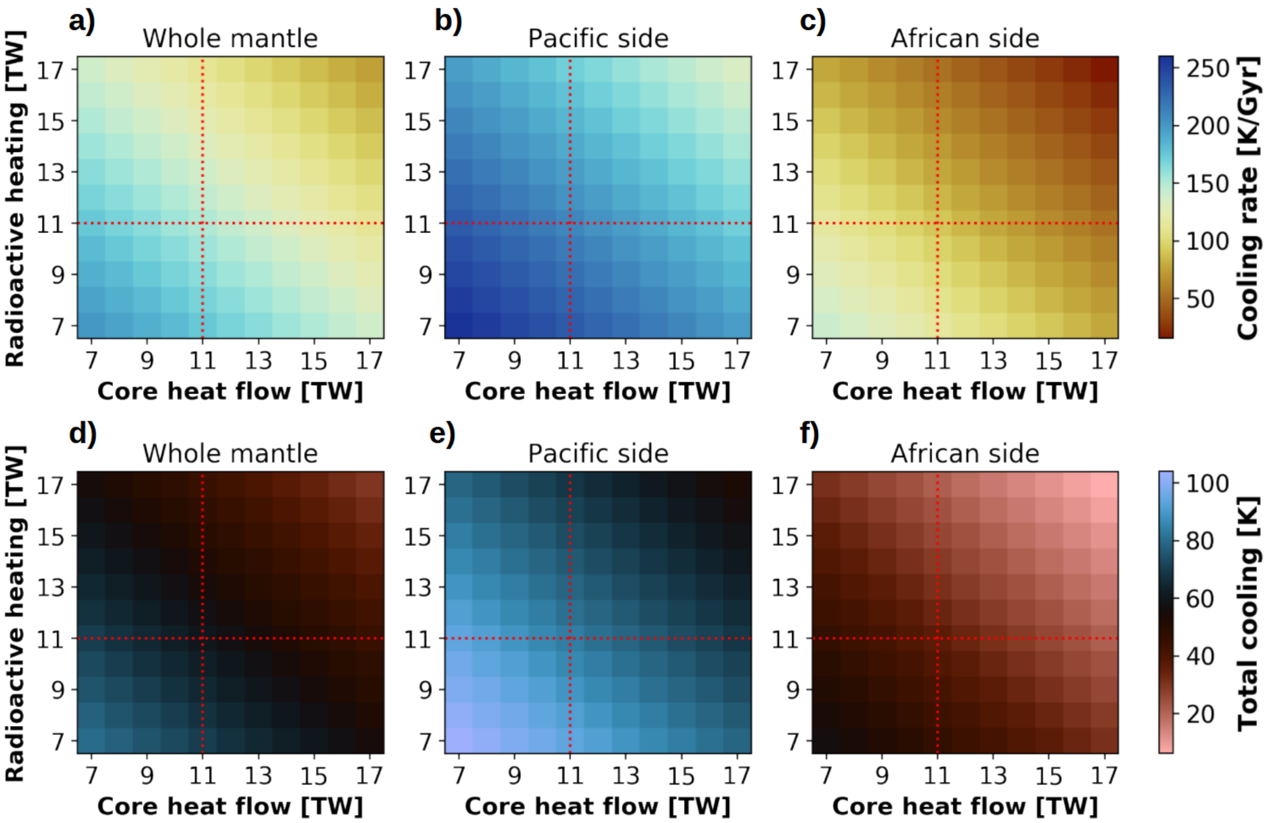

Figure S4: Time-averaged mantle cooling rates (a-c) and total mantle cooling (d-f) over the past 400 Myr for a range of radioactive heat production and core heat flow values. Note that the difference between all corresponding points in e) and f) is ~50 K, indicating that the resulting temperature difference between the Pacific and African mantle domains is independent of internal heat sources. Dashed red lines indicate the preferred values of mantle heat sources.

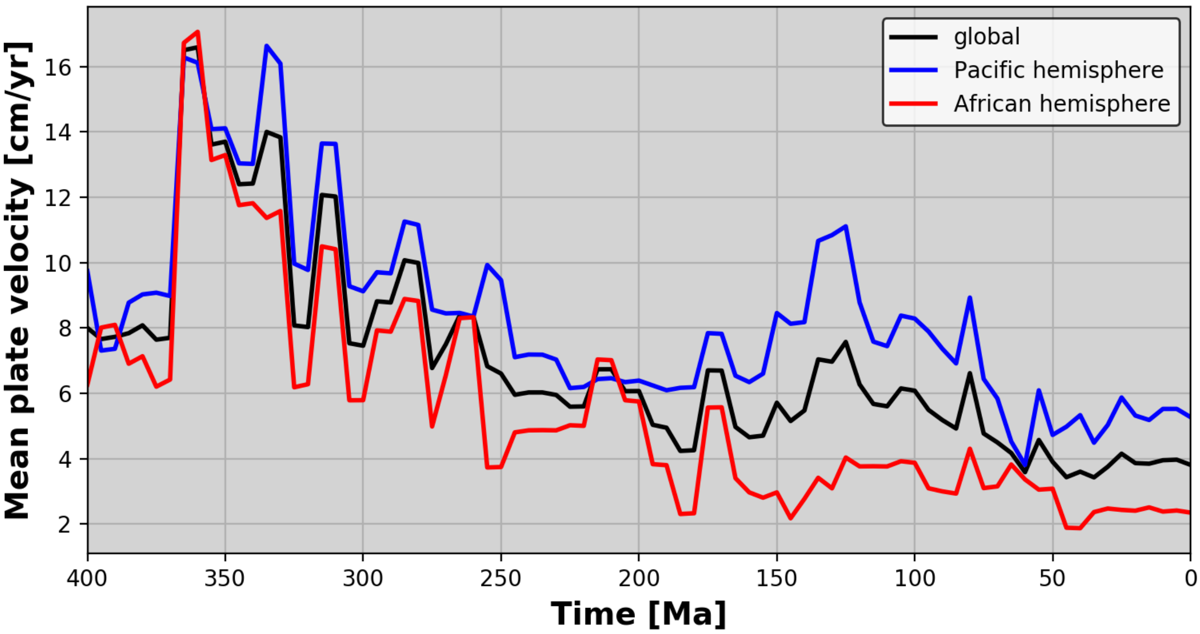

Figure S5: Mean plate speeds from the Pacific (blue) and African (red) hemispheres, compared to the global average (black). These are computed based on the plate tectonic reconstruction of Matthews et al. (2016), corrected after Torsvik et al. (2019).

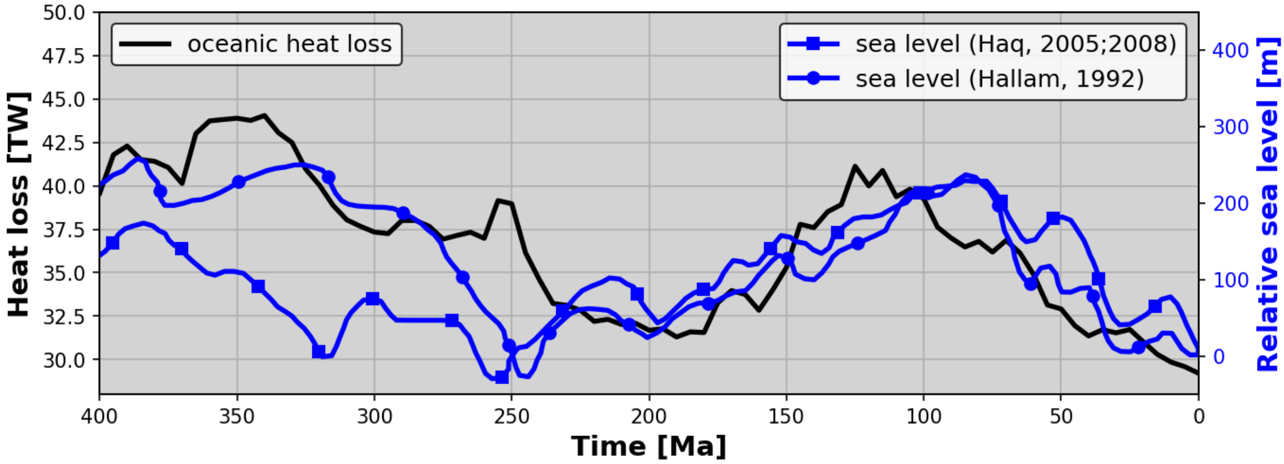

Figure S6: Time-dependence of oceanic heat loss (black line), calculated according to the description in Section 2 of the main text, and compared against the sea level record (blue lines, Hallam, 1992; Haq et al., 2005; Haq & Schutter, 2008).